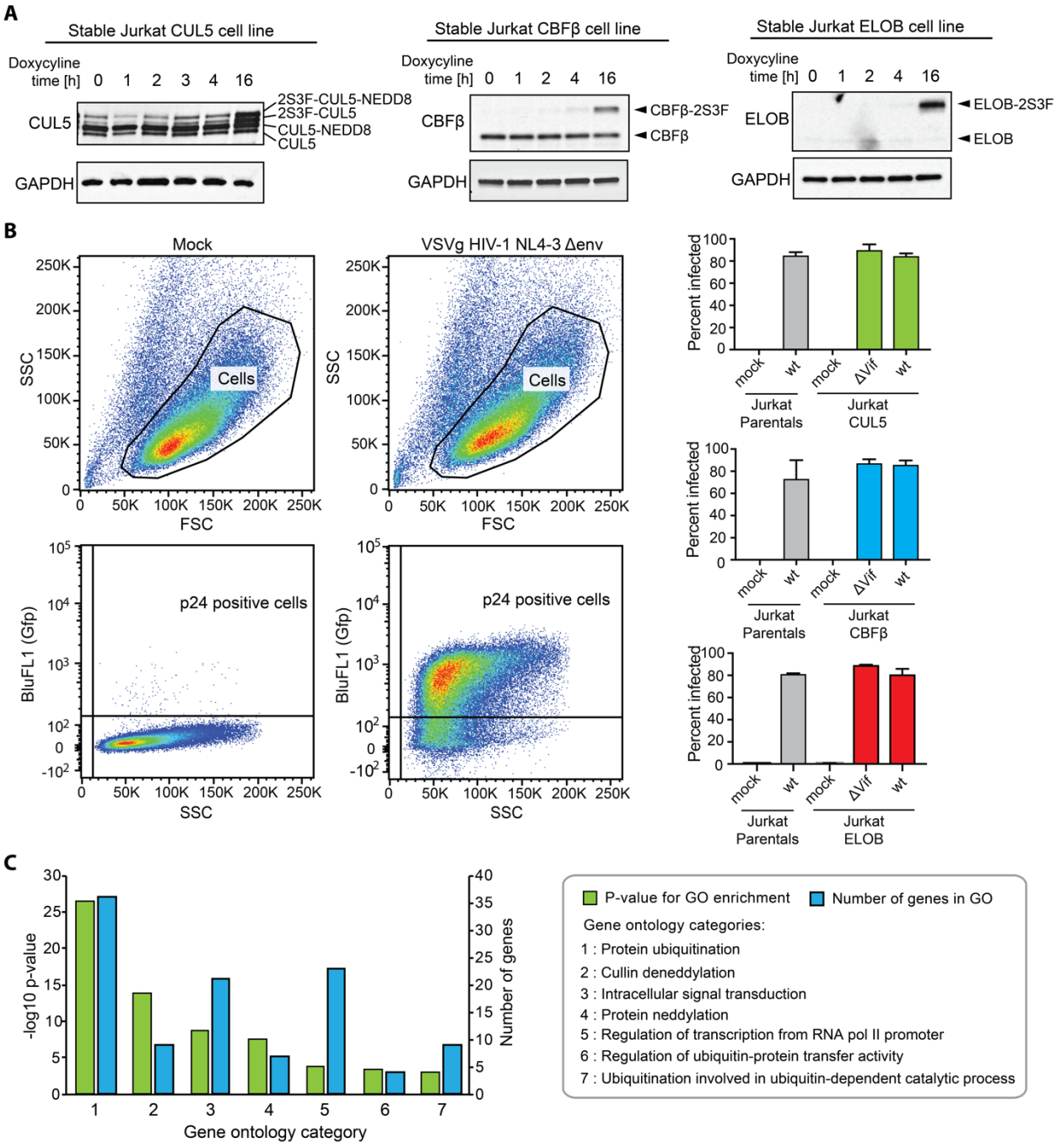

Figure S1. AP-MS quality controls, Related to Figure 2.

(A) Western blot analysis comparing the protein levels of endogenous CUL5, CBFß, and ELOB compared to 2xSTREP 3xFLAG (2S3F)-tagged version induced via tetracycline in Jurkat T cells

stably expressing each tagged factor. Time course was performed over 16 hours (overnight) and samples were taken after 1, 2, 3, 4, and 16 hours.

(B) Flow cytometry analysis of mock, HIV wt, and HIV ΔVif infected Jurkat T cells expressing affinity tagged proteins. Quantification was done by first gating on the live cell population, followed by gating on the $p24^+$ cells (n = 4; data from four replicate infections are presented as mean ± SEM).

(C) Gene ontology (GO) enrichment analysis for biological processes of validated CUL5, CBFß, and ELOB interactors performed using DAVID. Green bars indicate p-value for enrichment analysis and blue bars the number of genes represented in each GO category.

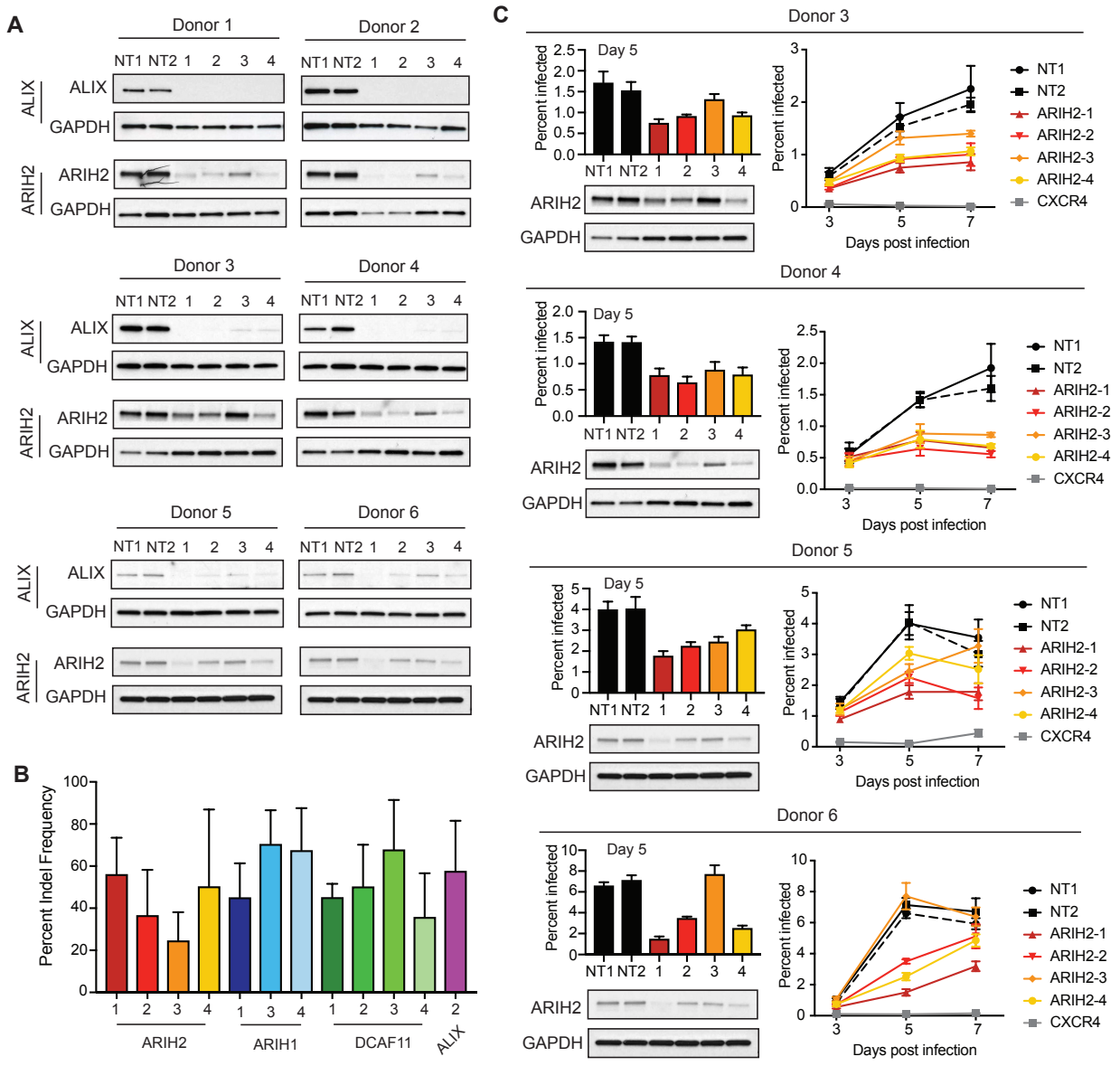

Figure S2. Knockout of selected Vif-dependent factors in primary T cells, Related to Figure 4.

(A) Western blots to assess CRISPR-Cas9 knockout efficiency of ARIH2 and ALIX in primary T cells derived from six different donors.

(B) Bar graph depicting mean percentage of insertion/deletion (indel) frequency determined by tracking of indels by decomposition (TIDE) analysis for various guide RNAs targeting ARIH2, ARIH1, DCAF11, and ALIX across six donors (n = 6, data are presented as mean + SEM).

(C) Western blots confirming ARIH2 knockout for all four guide RNAs in primary T cells from 4 donors and the corresponding HIV infection rate at day 5 of spread infection. HIV infection rate over 7 days for each donor is shown for each ARIH2 guide RNA compared to controls, non-targeting guide RNA and CXCR4 knockout (n = 3, data from three replicate infections are presented as mean ± SEM).

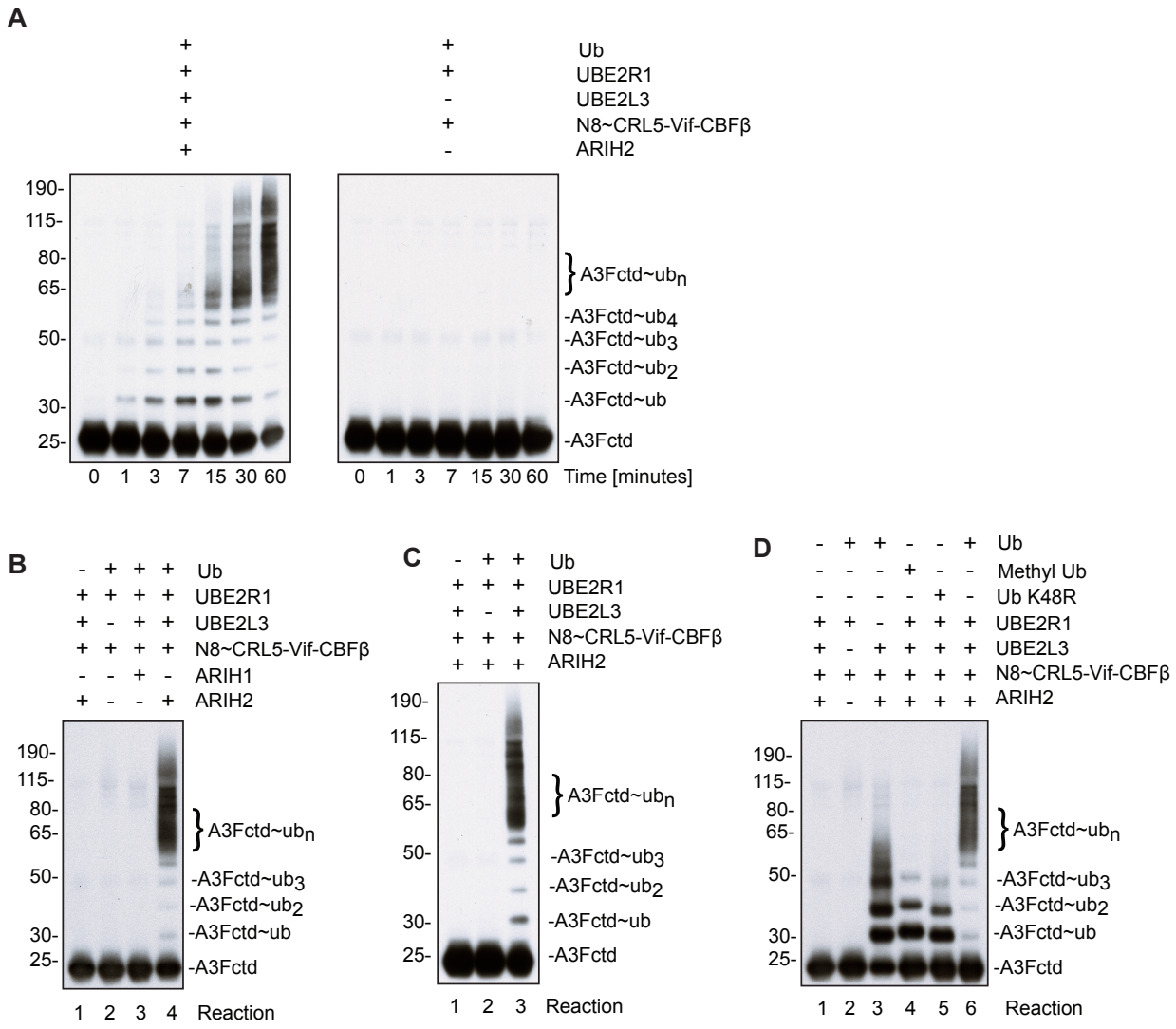

Figure S3. ARIH2 monoubiquitinates APOBEC3F to prime it for accelerated polyubiquitination via CUL5$^{Vif/CBFß}$ *in vitro*.

(A) Immunoblot showing time course for APOBEC3F C-terminal domain (APOBEC3Fctd) ubiquitination reactions in the presence and absence of ARIH2/UBE2L3. In the presence of ARIH2 and UBE2R1, formation of extensive ubiquitination chains on APOBEC3G via neddylated CUL5$^{Vif/CBFß}$ (N8~CRL5-Vif-CBFß) is accelerated and enhanced compared to treatment with neddylated CUL5$^{Vif/CBFß}$ and UBE2R1 alone.

(C) Acceleration of APOBEC3Fctd ubiquitination is specific for ARIH2 and cannot be phenocopied by replacing ARIH2 with ARIH1 (Reaction 3).

(D) Acceleration of APOBEC3Fctd ubiquitination is dependent on UBE2L3

(E) ARIH2 monoubiquitinates APOBEC3Fctd at multiple sites to prime for $CUL5^{vif/CBFß}$ dependent Ub chain extension. Immunoblot showing APOBEC3Fctd ubiquitination reactions in the presence and absence of UBE2R1, ARIH2 and $CUL5^{Vif/CBFß}$, Ub K48R, Methyl-Ub or wild-type Ub. Methyl-Ub (Reaction 4) and K48R-Ub (Reaction 5) recapitulate the pattern observed for the reaction that focuses on ARIH2 activity on A3G ubiquitination (Reaction 3, absence of UBE2R1).

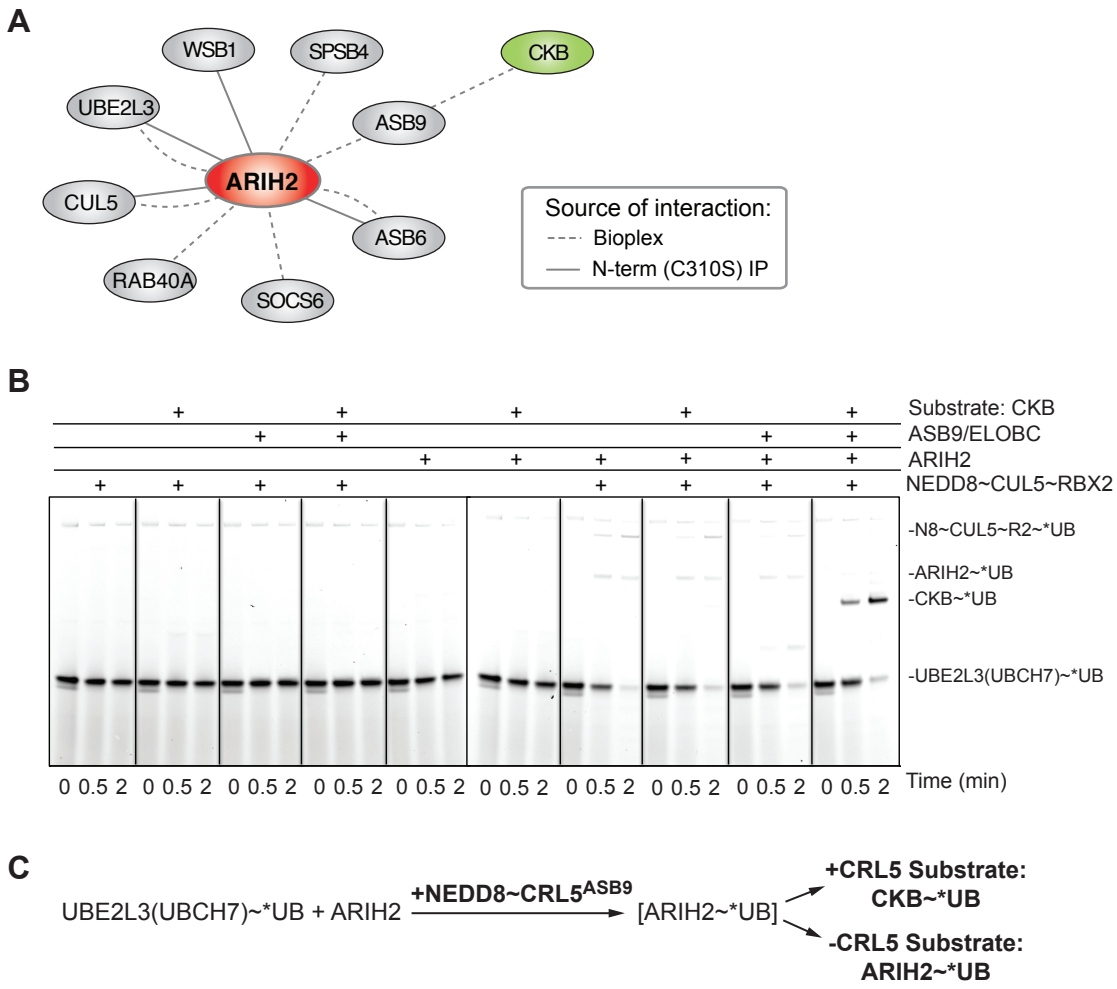

Figure S4. ARIH2 broadly interacts with components of the CRL5 complex and rapidly mediates Ub ligation to CRL5 substrate CKB, Related to Figure 7.

(A) High confidence interacting proteins for WT ARIH2 or catalytic C310S mutant.

(B) Fluorescent scans of gels of *in vitro* ubiquitination pulse-chase reaction. Pulse: thioester-linked UBCH7~*UB is generated and E1 reaction is quenched. Chase: ARIH2 is added; path of fluorescent UB* via ARIH2 is followed in presence or absence of neddylated CUL5-RBX2, the substrate receptor ASB9 and the CRL5 substrate CKB.

(C) Pathway inferred from (B): ARIH2 mediates Ub ligation to CKB depending on the neddylated CRL5 complex and the substrate receptor ASB9.